

OAK RIDGE NATIONAL LABORATORY LIBRARIES



3 4456 0548326 9

CENTRAL RESEARCH LIBRARY
DOCUMENT COLLECTION

ORNL-3684
UC-25 - Metals, Ceramics, and Materials
TID-4500 (34th ed.)

SOME OBSERVATIONS OF THE INTERGRANULAR
CORROSION OF IRRADIATED TYPE 304
STAINLESS STEEL

E. L. Long, Jr.
C. Michelson

CENTRAL RESEARCH LIBRARY
DOCUMENT COLLECTION
LIBRARY LOAN COPY
DO NOT TRANSFER TO ANOTHER PERSON
If you wish someone else to see this
document, send in name with document
and the library will arrange a loan.



OAK RIDGE NATIONAL LABORATORY
operated by
UNION CARBIDE CORPORATION
for the
U.S. ATOMIC ENERGY COMMISSION

Printed in USA. Price \$2.00. Available from the Clearinghouse for Federal
Scientific and Technical Information, National Bureau of Standards,
U.S. Department of Commerce, Springfield, Virginia

LEGAL NOTICE

This report was prepared as an account of Government sponsored work. Neither the United States, nor the Commission, nor any person acting on behalf of the Commission:

- A. Makes any warranty or representation, expressed or implied, with respect to the accuracy, completeness, or usefulness of the information contained in this report, or that the use of any information, apparatus, method, or process disclosed in this report may not infringe privately owned rights; or
- B. Assumes any liabilities with respect to the use of, or for damages resulting from the use of any information, apparatus, method, or process disclosed in this report.

As used in the above, "person acting on behalf of the Commission" includes any employee or contractor of the Commission, or employee of such contractor, to the extent that such employee or contractor of the Commission, or employee of such contractor prepares, disseminates, or provides access to, any information pursuant to his employment or contract with the Commission, or his employment with such contractor.

ORNL-3684

Contract No. W-7405-eng-26

METALS AND CERAMICS DIVISION

SOME OBSERVATIONS OF THE INTERGRANULAR CORROSION
OF IRRADIATED TYPE 304 STAINLESS STEEL

E. L. Long, Jr., and C. Michelson

NOVEMBER 1964

OAK RIDGE NATIONAL LABORATORY
Oak Ridge, Tennessee
operated by
UNION CARBIDE CORPORATION
for the
U.S. ATOMIC ENERGY COMMISSION



3 4456 0548326 9

SOME OBSERVATIONS OF THE INTERGRANULAR CORROSION
OF IRRADIATED TYPE 304 STAINLESS STEEL

E. L. Long, Jr., and C. Michelson¹

ABSTRACT

Five prototype instrumented fuel elements for the Experimental Gas-Cooled Reactor were irradiated in the helium-cooled ORR Loop 1 at cladding temperatures to 1500°F and burnups to 0.1 at. % U. These elements contained high-density, sintered UO₂ fuel bushings clad with type 304 stainless steel tubing.

During the postirradiation examination of certain of these test elements, some localized intergranular corrosion of the cladding was observed. In addition, extensive intergranular attack of type 304 stainless steel was detected in components operating adjacent to the test element but at lower temperatures (800-1200°F). This report discusses these observations and includes photographs and photomicrographs of typical corroded areas. The observations indicate that storage of sensitized, irradiated type 304 stainless steel in a high-humidity environment or underwater may lead to extensive intergranular corrosion.

INTRODUCTION

A number of irradiation experiments have been performed to test the fuel element concept for the Experimental Gas-Cooled Reactor being constructed by the Atomic Energy Commission at Oak Ridge. As a part of this irradiation program, five prototype instrumented fuel elements were irradiated in the ORR Loop 1 at clad temperatures to 1500°F and burnups to 0.1 at. % U. These elements, designated 5, 6, 7A, 7B, and 7C, contained high-density, sintered UO₂ bushings (0.707-in. OD × 0.323-in. ID × 0.375 in. long) and were clad with type 304 stainless steel tubing (0.710-in. ID × 0.020-in. wall). Each element was 19 in. long.

¹On loan to ORNL from the Tennessee Valley Authority.

The ORR Loop 1 is helium cooled and operates at 300 psia. A pictorial representation of the loop is shown in Fig. 1. After irradiation for one or two reactor operating cycles (50 or 100 days), each fuel element under test was transferred to a gas-filled storage tube in the ORR pool where it remained for a few weeks before postirradiation examination.

During the postirradiation examination of certain of these test elements, some localized intergranular corrosion of the cladding was observed. In addition, extensive intergranular attack was detected in type 304 stainless steel components operating adjacent to the test element but at lower temperatures (800-1200°F). The purpose of this report is to document and discuss these observations.

TEST PREPARATION AND IRRADIATION

The test fuel element and its associated components are shown in Fig. 2. Each test element was fabricated from preinspected type 304 stainless steel tubing having a nominal inside diameter of 0.710 in. and a wall thickness of 0.020 in. The chemical and physical properties of the tubing and end cap stock are listed in Table 1.

Each fuel element contained four thermocouples attached to the inner surface of the cladding and one fuel central-temperature thermocouple. The cladding thermocouples were copper brazed to the inner surface of the stainless steel tubing. The brazing was done in dry hydrogen for about 10 to 15 min at 2000°F. The central thermocouple well was a molybdenum-stainless steel assembly which was first copper brazed in a furnace and then welded to the top end cap by the gas tungsten-arc process. The top and bottom end caps were welded to the tubing by the gas tungsten-arc process. The thermocouple brazing cycle was the only extensive heat treatment of the tubing. A metallographic study was performed to verify that this heat treatment did not cause significant grain growth or carbide precipitation.

A summary of the five prototype fuel element tests including their operating conditions is presented in Table 2. The operating temperature for each test was controlled by the cladding thermocouple with the

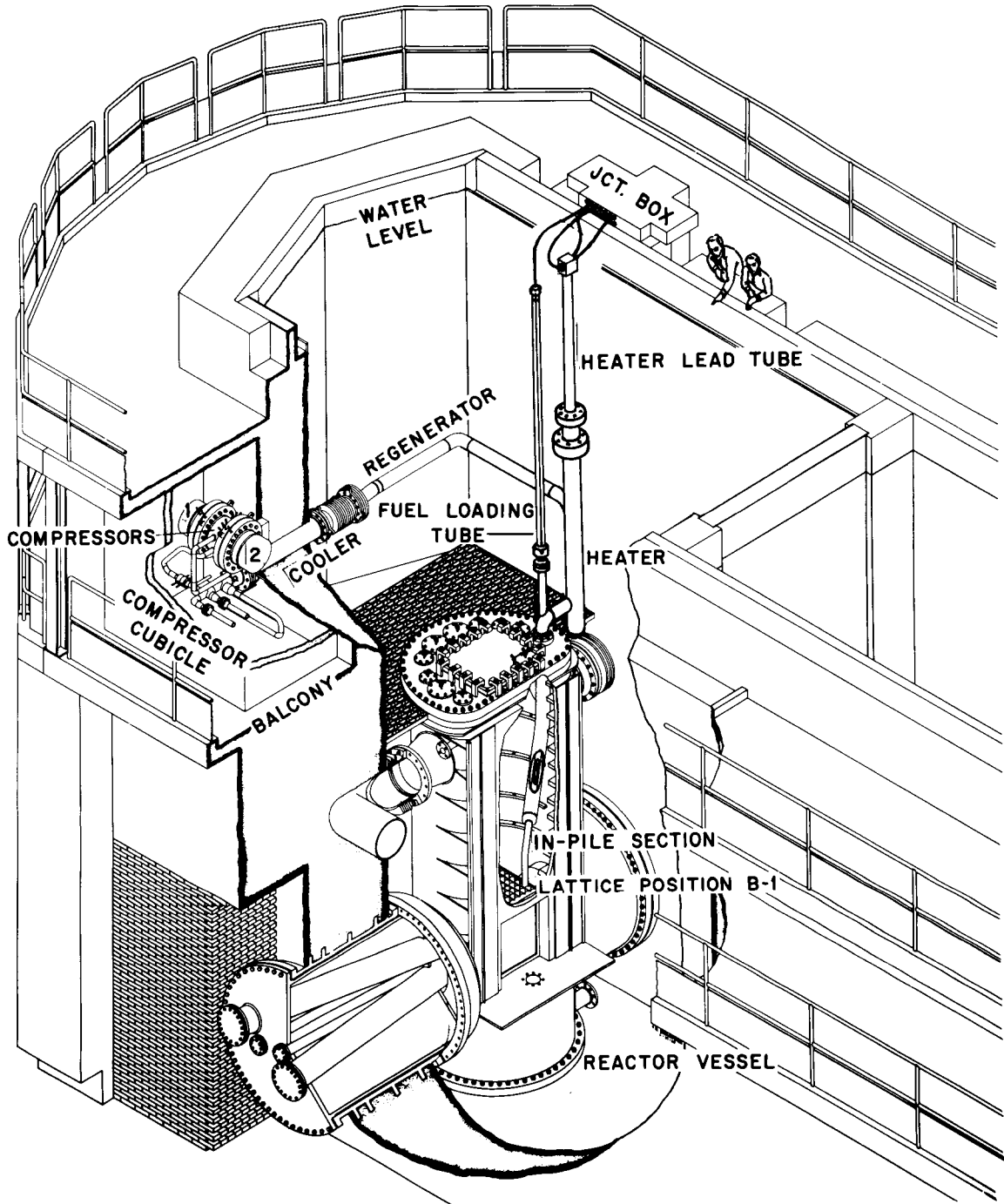


Fig. 1. Helium-Cooled Loop 1 at the ORR.

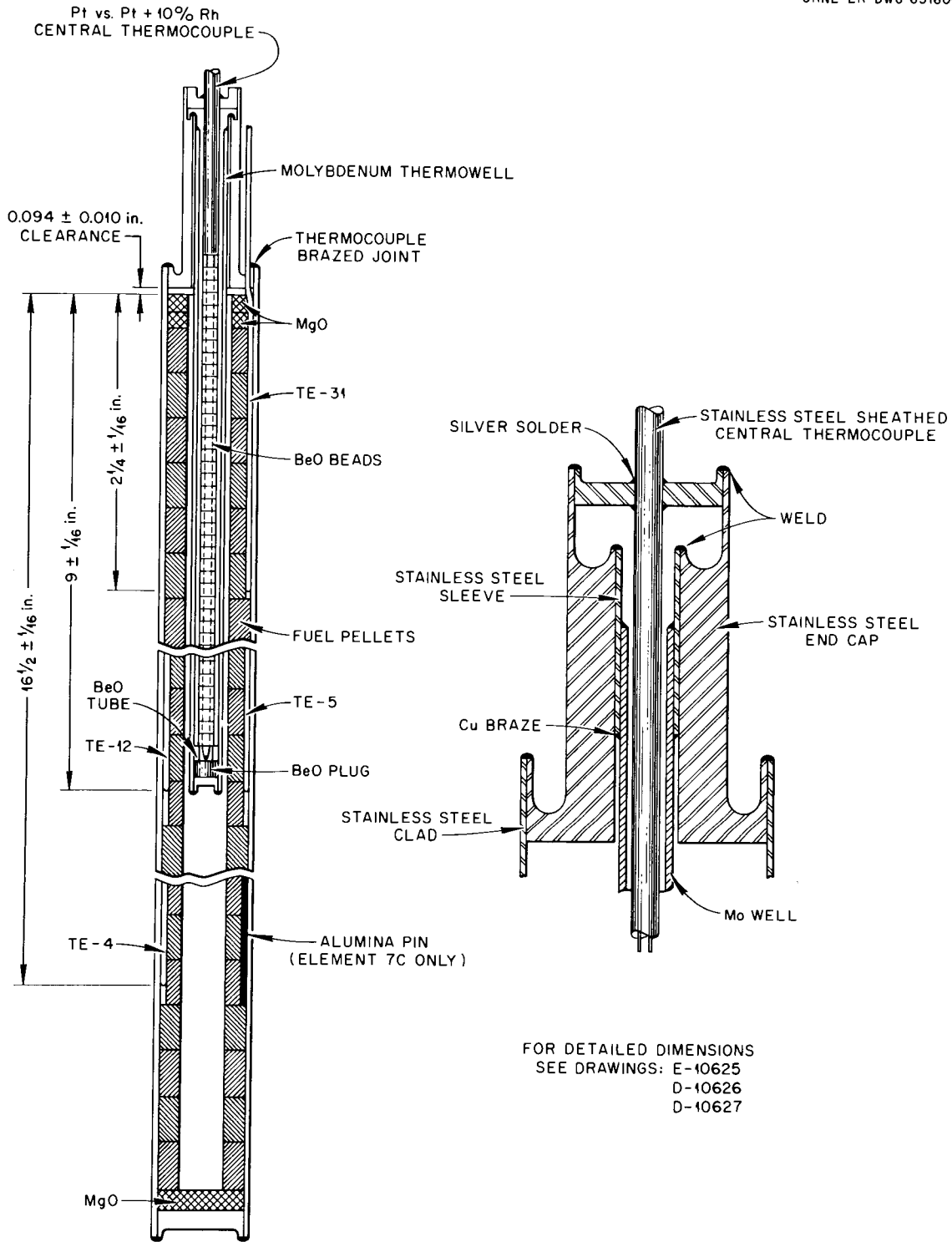


Fig. 2. Test Fuel Element for ORR Loop 1.

Table 1. Chemical Analyses and Mechanical Properties
of Type 304 Stainless Steel Components
for ORR Loop 1 Elements

Tubing				End Cap Stock	
Chemical Analysis ^a (wt %)		Mechanical Properties ^{a,b} (psi)		Chemical Analysis ^c (wt %)	
Carbon	0.05	Tensile Strength	90,200	Carbon	0.110 ^d
Manganese	1.61	Yield Strength	39,100	Manganese	1.07
Phosphorus	0.016			Silicon	0.50
Sulfur	0.006			Phosphorus	0.024
Silicon	0.38			Sulfur	0.013
Chromium	18.92			Chromium	18.01
Nickel	10.39			Nickel	9.00
Iron	Balance			Iron	Balance

^aManufacturer's analysis, Superior Tube Co., Heat No. 23999-X.

^bElongation per 2 in. is 57%.

^cORNL analysis No. 359.

^dThis material does not meet Metals and Ceramics Division Specifications MET-213 or MET-RM-A-276 because of excessive carbon content.

highest reading (or highest calculated temperature) and was not allowed to exceed a preset level. The gas inlet temperature was fixed by a preheater on the gas inlet line. The gas outlet temperature was fixed by the gas flow rate, inlet temperature, and power level of the test.

Each test element, except 7A, was contained in a type 304 stainless steel shroud tube that was attached to the element and fitted closely into the loop. The shroud extended the full length of the test element and was open at each end. Its purpose was to reduce the flow area around the test element, thus providing higher gas velocities and improved heat transfer to the helium. The shroud temperature was estimated to be about the same as the gas temperature.

The shroud of element 7A was replaced by an insert of similar design which was placed directly into the loop piping. The chemical and physical properties of the shroud and insert material used for

Table 2. Summary of Prototype EGCR Instrumented Fuel Element Tests in ORR Loop 1

	Fuel Element Number				
	6	5	7A	7B	7C
Date inserted into loop	9-3-61	11-1-61	12-22-61	2-19-62	4-17-62
Date removed from loop	10-22-61	12-17-61	2-11-62	4-8-62	7-29-62
Date removed from ORR storage	11-22-61	1-30-62	3-1-62	5-1-62	8-13-62
Time in ORR storage (days)	31	44	18	23	15
Date of final examination	12-5-61	2-9-62	3-21-62	6-18-62	9-13-62
Heat rating ^a (Btu/hr·ft)	23,000-26,000	18,000-23,000	26,000-28,000	25,000-28,000	25,000-28,000
<u>Average Operating Temperatures (°F)</u>					
Cladding					
Maximum (bottom)	1405	1450 ^b	1100-1500 ^c	d	1535
Minimum (top)	1100-1225	900-1100	900	1300-1350	1265-1415
Gas inlet	1025	925	550-650	870	870-900
Gas outlet ^e	1140	1060	660-770	1130	1055-1065
Central Fuel	1500-1950	1790-1840	1650-2050	d	2000-2200

^aThermal neutron flux was approximately 3 to 4 × 10¹³ neutrons/cm²·sec.

^bEstimated.

^cMidplane temperature - bottom thermocouple failed.

^dThermocouple failed.

^eDoes not reflect peak values of short duration.

each test element are given below. The only extensive heat treatment of the shroud or insert tubing was a copper brazing cycle to 2000°F for about 10 to 15 min to attach some thermocouples and spacers.

Type 304 Stainless Steel^a Shrouds and Inserts
for ORR Loop 1 Elements

Chemical Analysis ^b (wt %)		Mechanical Properties ^{b,c} (psi)	
Carbon	0.062	Tensile Strength	89,350
Manganese	1.71	Yield Strength	46,860
Phosphorus	0.011		
Sulfur	0.010		
Chromium	18.65		
Nickel	10.43		
Molybdenum	0.23		
Copper	0.12		
Silicon	0.61		
Iron	Balance		

^aType 304 stainless steel seamless aircraft tubing (1-in. OD × 0.020-in. wall) to Specification MILOT - 8504.

^bManufacturer's analysis, Pacific Tube Co., Heat No. 26842.

^cElongation per 2 in. is 55.0%.

POSTIRRADIATION PROCEDURES

After irradiation, each test element was removed by retracting it into the fuel loading tube shown in Fig. 1. The loading tube was then isolated and removed by closing two valves located at the bottom end and breaking the flanged connection between them. The top end was closed with a blind flange, and the tube was pressurized to about 20 psig with nitrogen. The tube was then sealed off and transferred to an underwater storage area. During storage, the test element was exposed to the overpressure of nitrogen plus the original atmosphere of air and unknown amounts of water vapor due to leakage or other sources.

Following a storage period of several weeks, the loading tube was transferred to a hot cell at one end of the ORR pool. Here the experiment was removed from the tube (see Table 2 for date of removal from the ORR storage). Appendages such as the lead tube and thermocouples

were cut off a short distance above the shroud, and in some cases the shroud was removed. The test element and its shroud were placed in an air-filled carrier for transfer to a hot cell in another building. At their final destination, some of the elements were placed in sealed brass cans and stored for an additional time before being examined. The date of final examination in a hot cell is indicated in Table 2.

The only exception to the above procedure was test element 7A. In this case, the insert (shroud) was removed after the test element was retracted into a fuel loading tube and disconnected from the loop. The insert was removed by retracting it into another loading tube, disconnecting the tube from the loop, and then removing the insert for storage directly in the ORR pool water.

After a given test element reached a hot cell for final examination (see Table 2 for date), it was removed from its carrier or brass storage can and disassembled. The first step was to remove the shroud (if it had not been removed previously) and visually inspect the shroud and test element. The remaining examination included gamma scanning, dimensioning, leak checking, puncturing for fission-gas analysis, and then sectioning of the test element for metallographic investigation and burnup determination. The shroud did not receive additional examination unless the visual inspection indicated a need for metallography.

POSTIRRADIATION OBSERVATIONS

During the postirradiation examination of certain test elements, some localized intergranular corrosion of the cladding and extensive intergranular corrosion of the shrouds and other capsule components was observed. These observations are detailed below.

Test Element 5

A visual examination of the cladding for test element 5 showed no severe deformation or reactions. There was a slight rust-colored area on the cladding at the bottom of the element. Small pits containing a corrosion product were also observed. The element was sectioned at the discolored areas for metallographic examination. Localized intergranular attack was noted at the outer surface of the cladding to depths

of 2 and 4 mils in specimens from the top and bottom of the fuel element, respectively. No chemical reaction products were observed.

During visual examination, both the shroud covering the test element and the remaining section of lead tube from which the element was originally suspended were found to be covered with a rust-colored corrosion product. Although handled carefully, the lead tube fractured at two points, 6 1/2 and 21 in. above the joint between the lead tube and shroud (see Fig. 3). The thermocouple leads can be seen inside the lead tube. The larger tube in this figure is the stainless steel shroud. Both fractures appeared to be brittle.

The corrosion product from both the lead tube and shroud was collected and analyzed. The analysis indicated that both samples had the same composition. X-ray analysis indicated the products to be gamma-Fe₂O₃·H₂O. Semiquantitative spectrographic analysis showed that the oxide contained iron, chromium, and nickel in quantities greater than 1% and that Bi, Zn, Sn, Au, Ag, Mn, Mo, Al, Cu, and Si were present in trace quantities (listed in decreasing order of the amount present).

A section of unirradiated type 304 stainless steel tubing thought to be from the same heat that was used in the fabrication of the lead tube for element 5 was examined metallographically. A microstructure typical of type 304 stainless steel was observed, and no evidence of any abnormalities was seen. The average microhardness was 185 DPH.

The extreme friability of the lead tube after irradiation was demonstrated when a sample from near one of the fractures was mounted in Bakelite for metallographic examination. During the subsequent lapping and polishing, grains fell out of the sample (see Fig. 4). Another sample was mounted in epoxy resin, thus requiring no pressure. It is shown in Fig. 5. Grain boundary separation was "spotty" rather than general and originated at the outer surface of the tubing in all instances. Intergranular fracturing extended through the tube wall in several areas. Microhardness measurements revealed a maximum hardness of 200 DPH, which negated the possibility of general embrittlement of the microstructure even though embrittlement had obviously taken place in the grain boundaries. Some transgranular fracturing was observed in

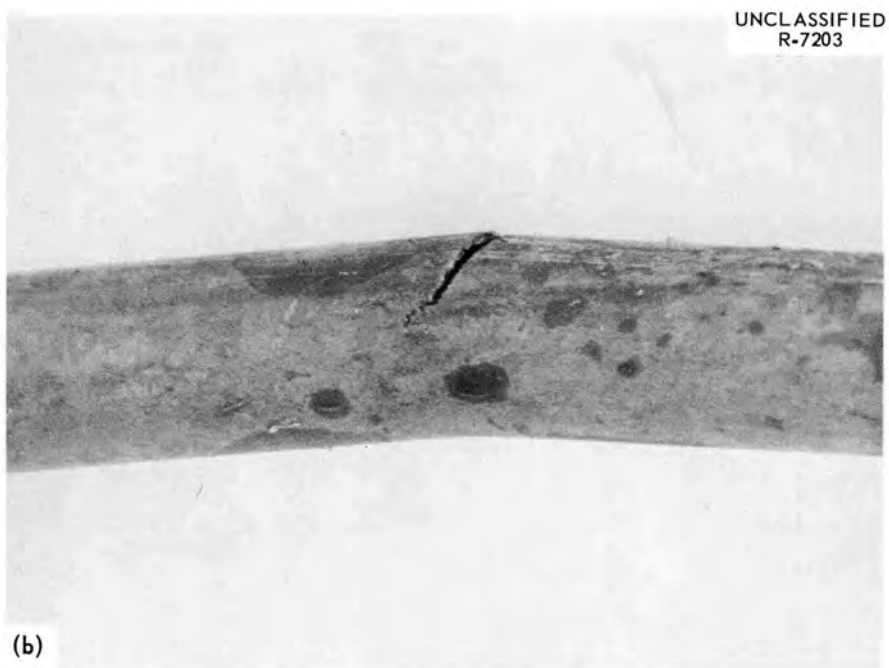
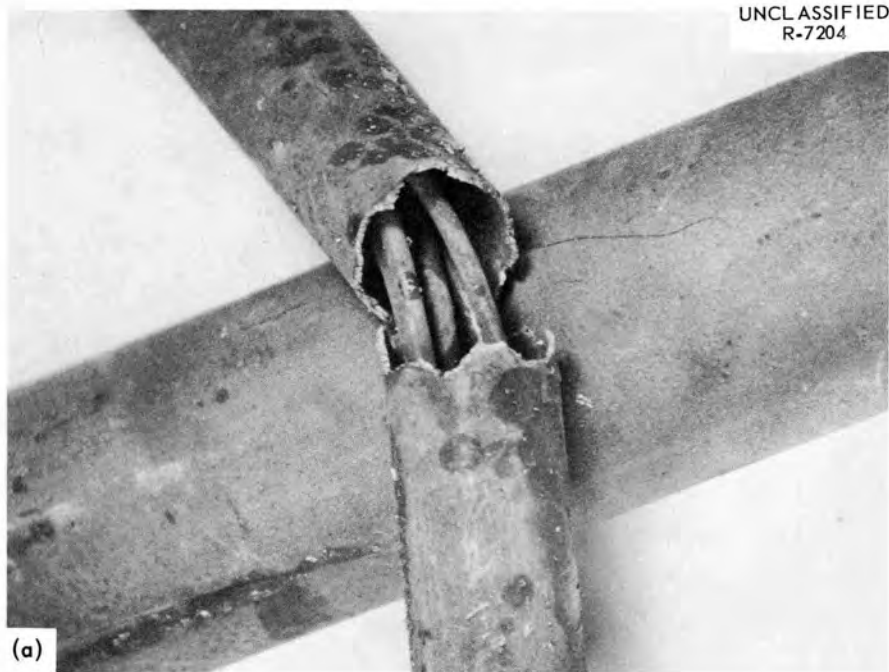


Fig. 3. Fractures in Type 304 Stainless Steel Lead Tube for Test Element 5. Fractures Occurred Approximately (a) 6 1/2 in. and (b) 21 in. Above the Test Element.



Fig. 4. Bakelite-Mounted Transverse Sample Taken from Near a Fracture in the Type 304 Stainless Steel Lead Tube for Test Element 5. As-polished; 100X. Reduced 12%.



Fig. 5. Epoxy-Mounted Transverse Sample Taken from Near a Fracture in the Type 304 Stainless Steel Lead Tube for Test Element 5. As-polished; 100X. Reduced 12%.

the epoxy-mounted sample (see Fig. 6), but intergranular failure was the predominant mode of fracture propagation. Examination of the fractures in this sample at high magnification revealed the presence of a corrosion product that appeared to be an oxide (see Fig. 7).

Transverse sections were cut through the shroud opposite points near the midlength and bottom of the test element. The section from near the midlength revealed localized intergranular attack primarily at the inner surface and to a maximum depth of 2 to 3 mils (see Fig. 8a). The section of shroud from near the bottom revealed severe intergranular attack, and in several places intergranular fractures penetrated the entire wall (see Fig. 8b). In general, this specimen was similar in appearance to the lead tube.

Test Element 7A

A type 304 stainless steel insert was used for test element 7A in place of the shroud normally used for controlling gas flow. After irradiation, this insert was stored in the ORR pool instead of the fuel loading tube. The bottom portion of the insert, which was irradiated at an average temperature above 770°F (gas outlet temperature), rusted badly while in pool storage. A longitudinal fracture developed at the bottom of the insert while being sectioned for a metallographic specimen (see Fig. 9). A metallographic examination of the specimen revealed an intermittent oxide that penetrated the outside diametral surface to a maximum depth of 0.5 mil (see Fig. 10a). Metallographic examination of the crack that developed during sectioning revealed severe intergranular separation and evidence of an intergranular corrosion product in the fracture region (see Fig. 10b).

Transverse sections were taken from the middle and approximately 3 in. from the middle of the test element to determine the nature of a dark ring observed near the midlength of the element and the integrity of the braze between the thermocouple sheath and the cladding. Examination of the specimen from the middle of the element revealed a tightly adhering oxide that penetrated the outer surface of the cladding to a maximum depth of 1.5 mils (see Fig. 11a). The specimen taken approximately 3 in. from the middle of the element revealed a spotty oxide that



Fig. 6. Transverse Section Through the Lead Tube of Test Element 5 Showing both Inter- and Transgranular Fractures. Etchant: aqua regia; 500X. Reduced 12%.

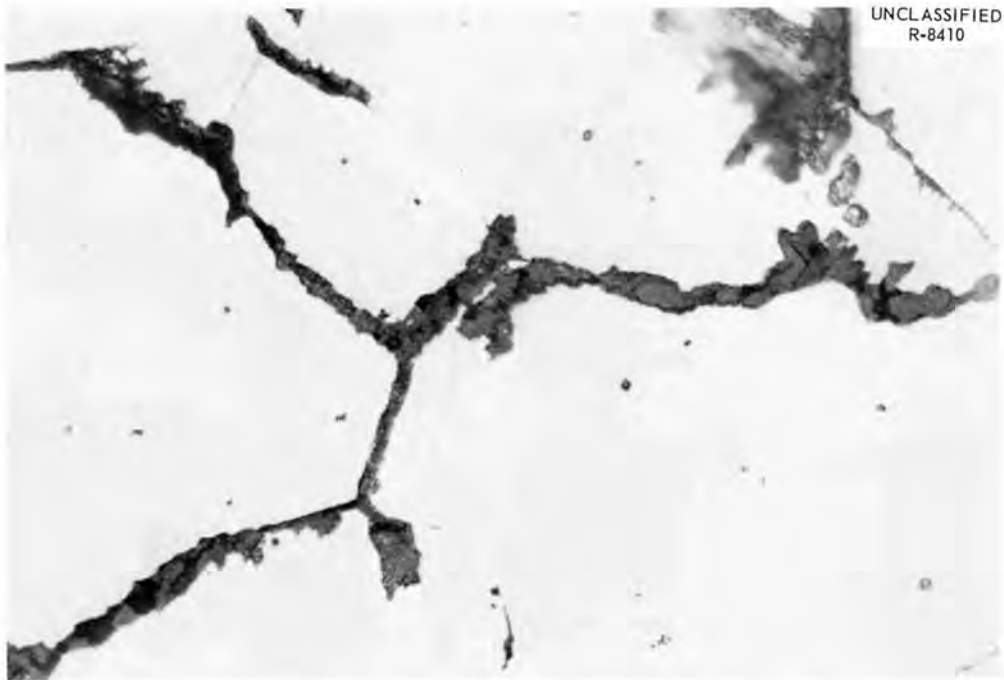


Fig. 7. Corrosion Product in the Fractures of the Transverse Section Through the Lead Tube of Test Element 5. As-polished; 1000X. Reduced 12%.



Fig. 8. Transverse Sections Through (a) Midlength and (b) Bottom of the Shroud for Test Element 5. As-polished; 150X.

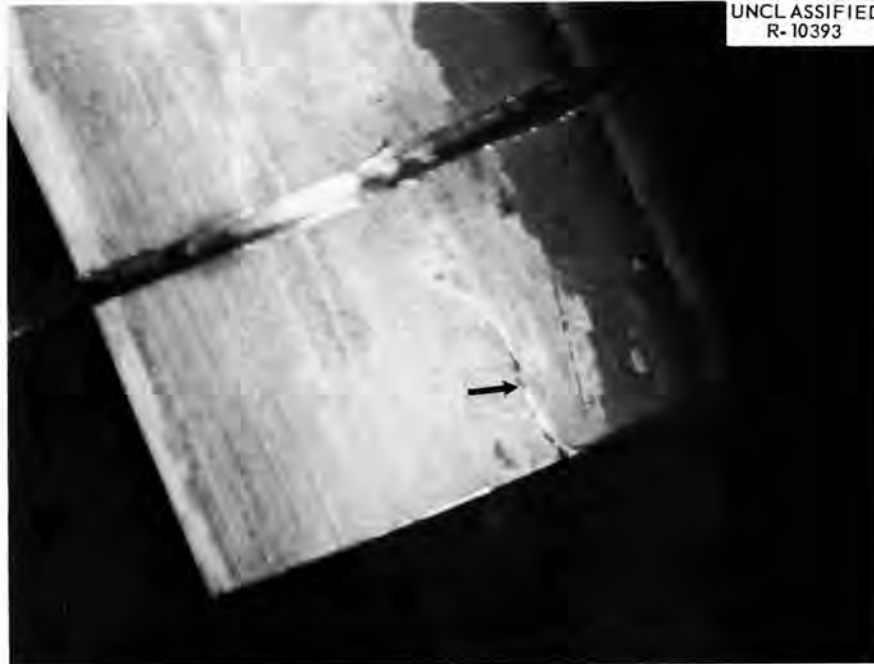


Fig. 9. Longitudinal Crack that Appeared While Sectioning the Insert for Test Element 7A.

penetrated the outer surface of the cladding to a maximum depth of 0.5 mil (see Fig. 11b). Also, a large variation in grain size was noted in both specimens. There were some areas where only two grains existed across the wall of the cladding. The large grains present after irradiation are the result of germinative grain growth. Profile measurements of this element indicated the maximum bow was in the region where the metallographic specimens were taken. The areas of large grain size were not related to the thermocouple sheath-to-cladding brazed joints. A metallographic study of similar unirradiated tubing which had been through a thermocouple brazing cycle disclosed a fine-grained microstructure.

Test Element 7C

A visual examination of the shroud for test element 7C indicated a loosely adhering rust-colored corrosion product over its entire length (dull areas in Fig. 12) except for the screw threads and spacing ring. Some water was present in the loading tube, and there were rust-colored contour lines on the shroud (see Fig. 13). These lines were attributed

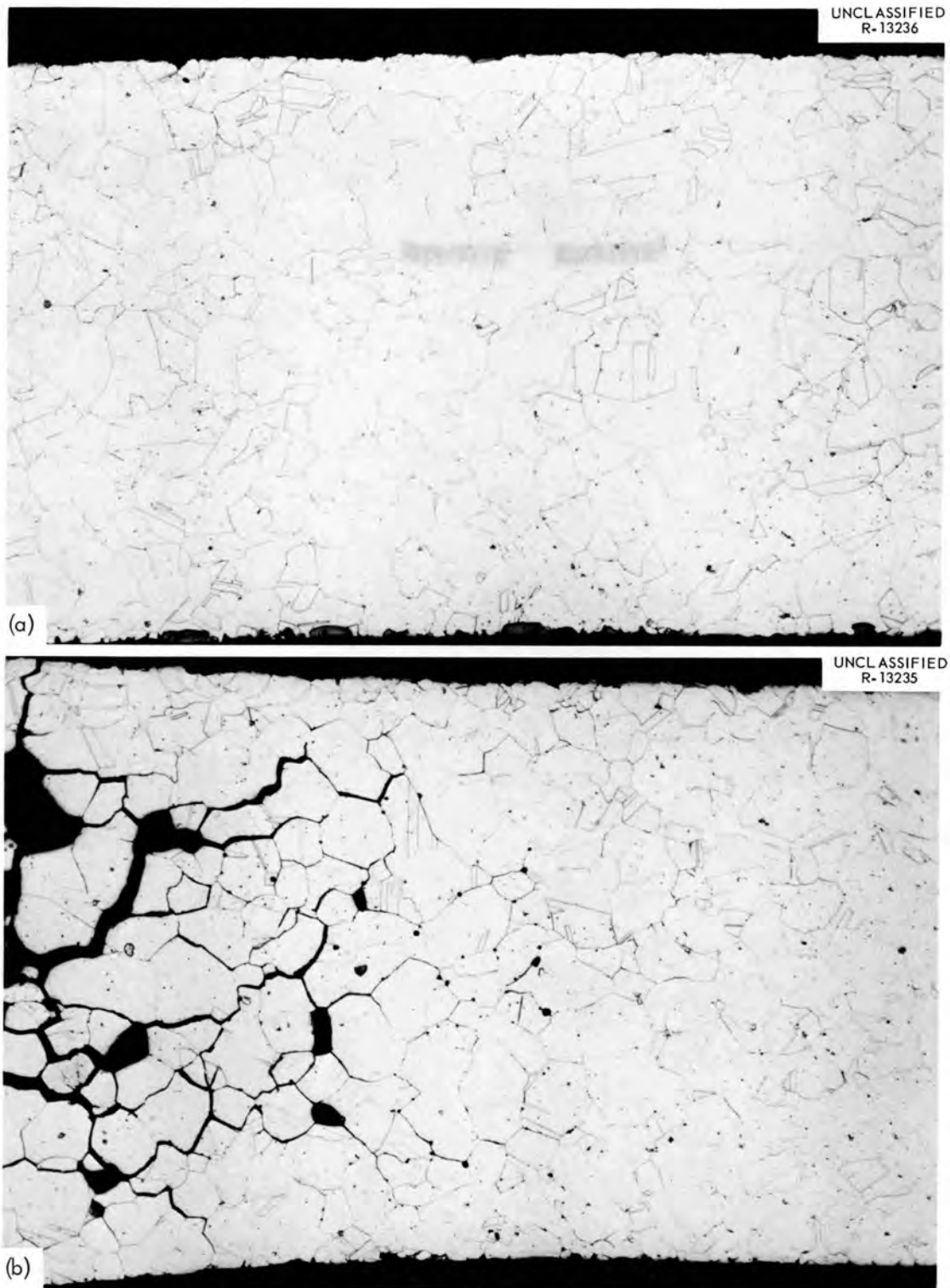


Fig. 10. Transverse Section Through Bottom on Insert for Test Element 7A Showing (a) Intermittent Oxide on Surface and (b) Intergranular Separation. Etchant: aqua regia; 200X. Reduced 11%.

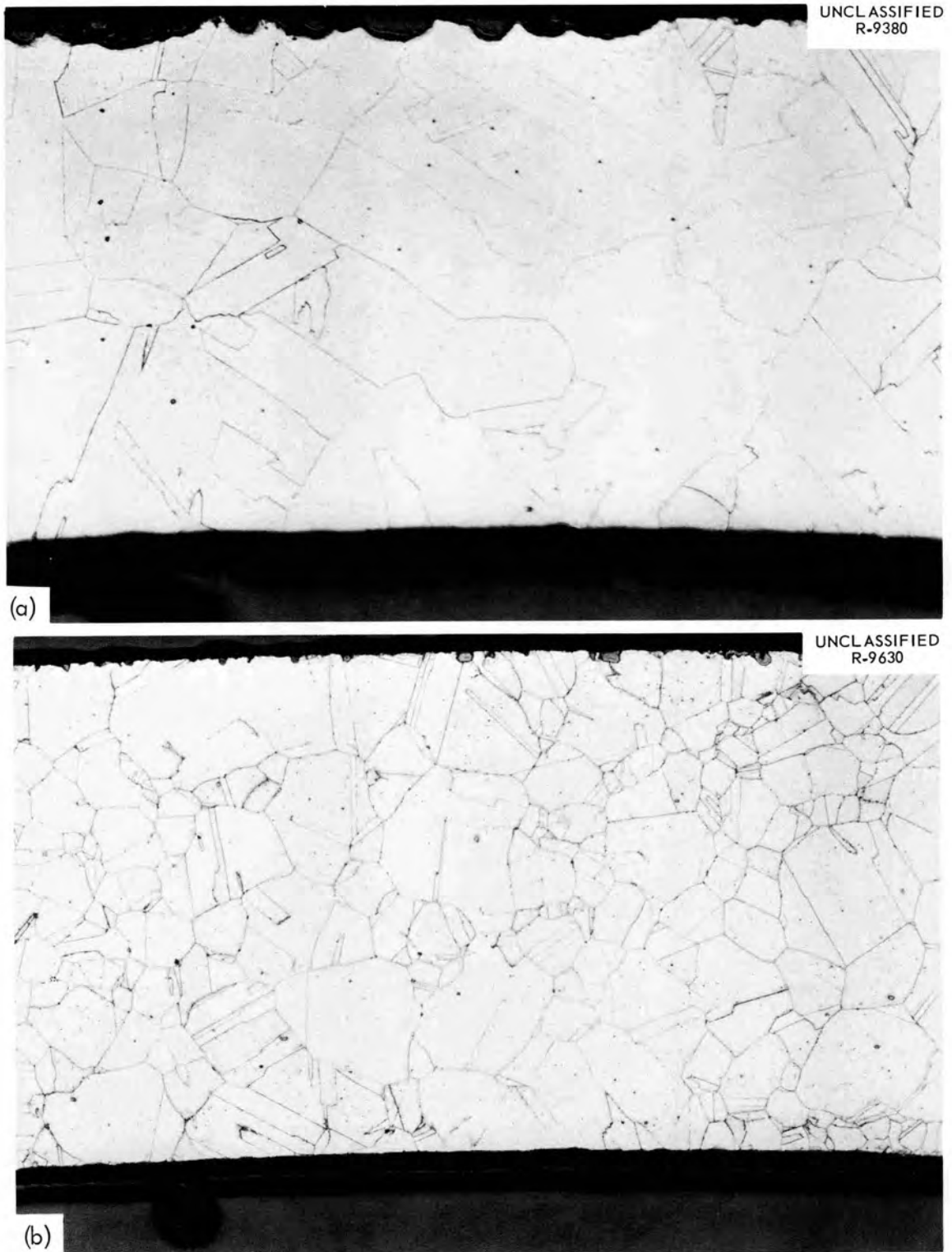


Fig. 11. Transverse Sections Taken from (a) Middle and (b) 3 in. from Middle of Cladding for Test Element 7A. Etchant: glyceria regia; 150X.

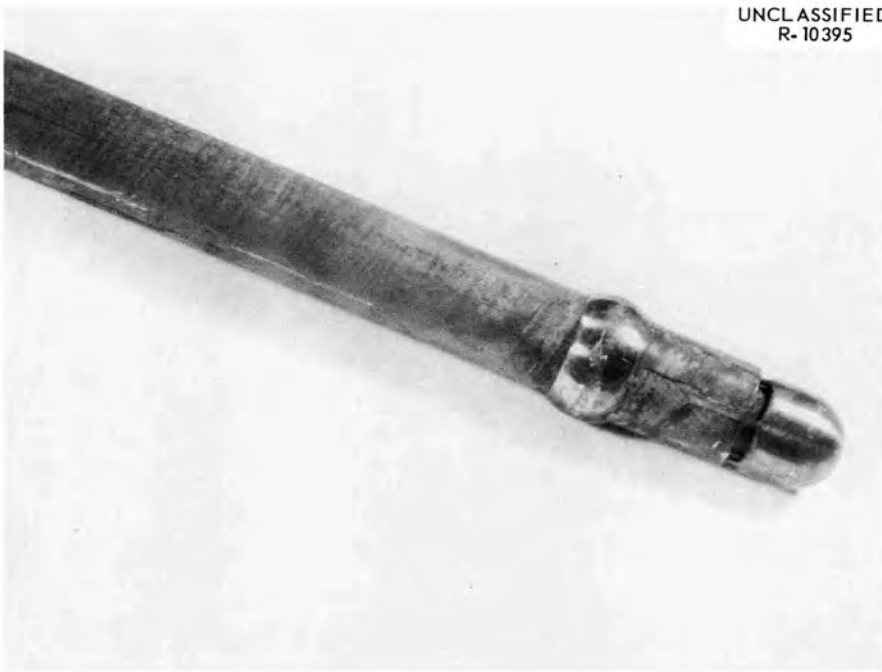


Fig. 12. Type 304 Stainless Steel Shroud for Test Element 7C.

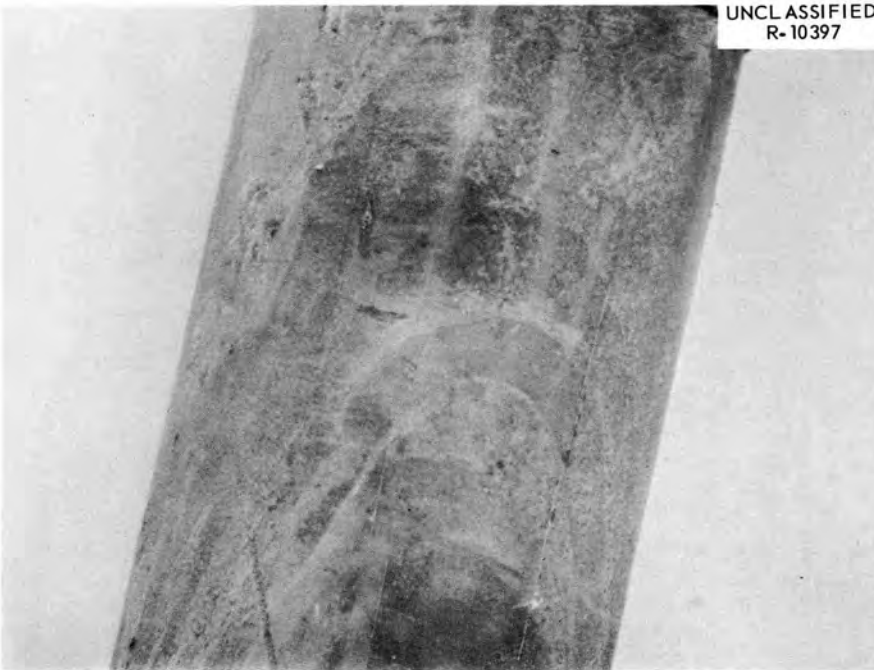


Fig. 13. Rust-Colored Contour Lines on the Shroud for Test Element 7C.

to different water levels caused by changes in position of the tube while in the reactor pool. A transverse section was made at the bottom of the shroud and prepared for metallographic examination. A lack of grain boundary integrity resulted in grains falling out from the inside diametral regions during metallographic preparation (see Fig. 14). This lack of grain boundary integrity in the shroud was sporadic and was observed in only three areas of the specimen.

The general appearance of the cladding for element 7C was good, although there were light rust-colored spots near the top and bottom of the element. No changes in the diameter or length of the cladding were observed. However, a bow of 40 mils was measured in the central portion. Four leaks were found in the element by means of a vacuum oil test (element was immersed in an evacuated cylinder containing silicon oil). Two leaks were found $1/4$ in. below the top end cap and two were found about $3\ 1/2$ in. above the bottom end cap. Specimens were cut from these areas for metallographic examination. A transverse section through the capsule at the interface between the top fuel pellet and the MgO insulators revealed two regions where intergranular failure had occurred (see Fig. 15). The failures were similar in appearance to those seen in the shrouds of elements 5 and 7C except that there was no evidence of a corrosion product in the intergranular fractures in the element 7C cladding. Furthermore, the cladding failures began at the inner surface and differed from those seen in the shrouds in that the inner surface of the cladding had not been exposed to water during storage. The failures did not appear to be associated with the copper used to braze the internal thermocouples to the cladding since regions were seen where the copper had penetrated the cladding intergranularly but the cladding remained intact.

A fine and apparently continuous precipitate was observed along the grain boundaries in the metallographic specimen obtained from the top portion of test element 7C (see Fig. 16). The intergranular precipitate in a specimen from near the midlength of the same element appeared discontinuous (see Fig. 17). A specimen was prepared for x-ray diffraction in an attempt to identify the precipitates. Even though the precipitates were put in relief by etching, the pattern obtained was too weak for identification.



Fig. 14. Area from Bottom Portion of the Shroud for Test Element 7C Showing Lack of Grain Boundary Integrity at the Inside Diameter. Etched; 200X.

Other Test Elements

Since there were no indications of either clad failures or chemical reactions between fuel and cladding for test element 6, no metallographic samples were selected for examination. There were no visual indications of shroud failure. A visual examination of test element 7B indicated that no extensive attack of the shroud or cladding had occurred during irradiation; therefore, no metallography was performed.

DISCUSSION

Intergranular corrosion of type 304 stainless steel was observed in the shrouds of elements 5, 7A, and 7C. The corrosion appeared following two distinctly different modes of storage. The shrouds for elements 5 and 7C were stored in air with a nitrogen overpressure while the insert (shroud) for element 7A was stored directly in the ORR pool

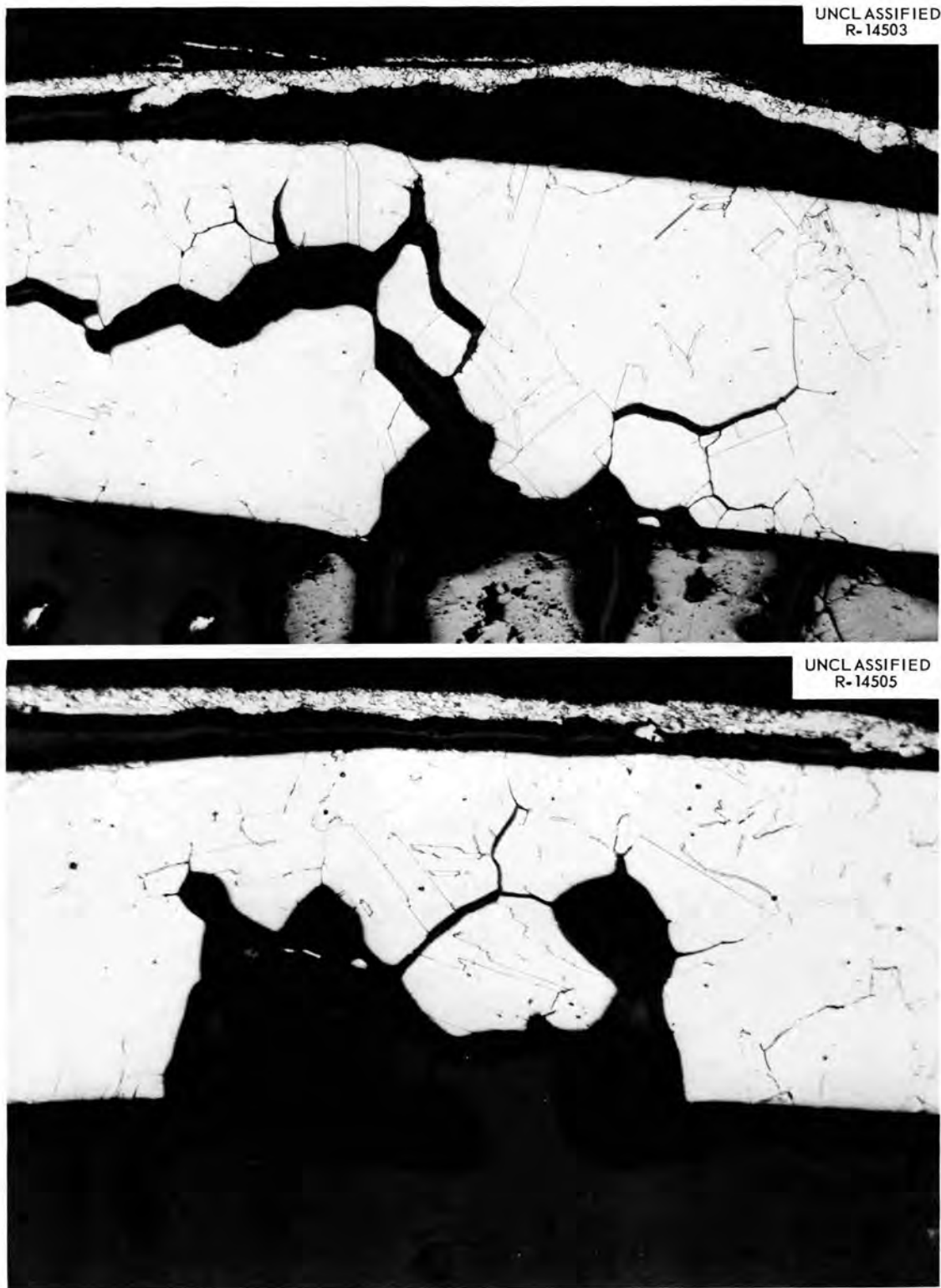


Fig. 15. Areas from a Transverse Section from Test Element 7C Showing Intergranular Cladding Failures at Interface Between Top Fuel Pellet and MgO Spacer. Etched; 100X.

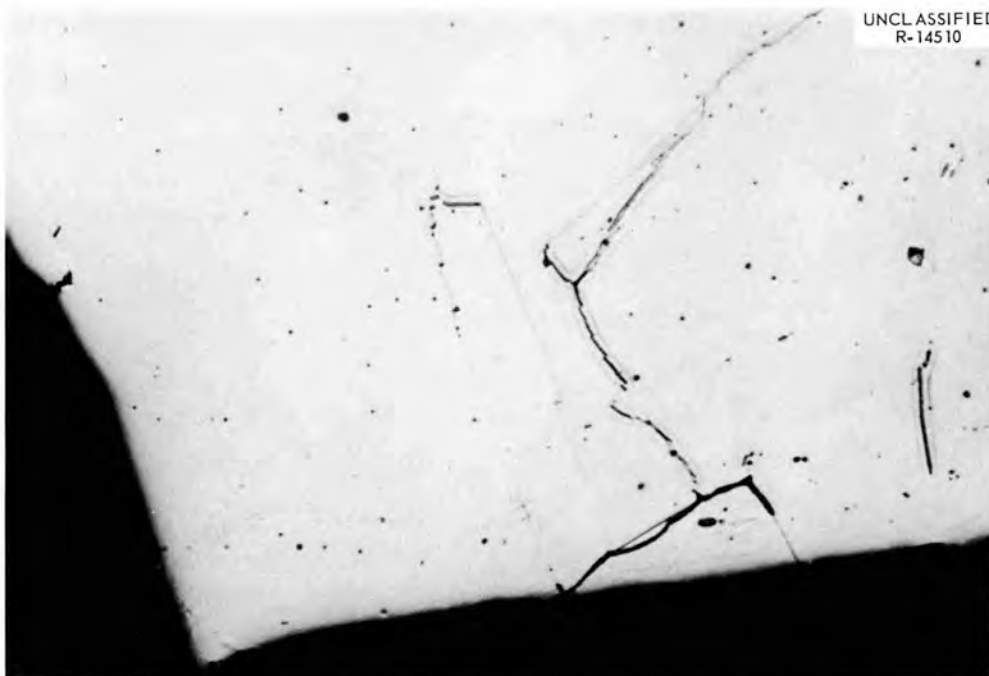


Fig. 16. Transverse Section from Top Portion of Test Element 7C Showing Fine and Apparently Continuous Precipitate Along Grain Boundaries. 500X. Reduced 12%.



Fig. 17. Transverse Section from Near Midlength of Test Element 7C Showing Discontinuous Precipitate Along Grain Boundaries. Etched; 500X. Reduced 12%.

water. Further, the corrosion did not appear attributable to the presence of a high external radiation field since the insert for element 7A did not have a test element attached during storage in the pool. For this case, the only significant radiation present must have come from neutron-induced activity in the stainless steel. The shrouds for the other elements remained attached to their respective test elements during pool storage. As a result, they were exposed to a strong gamma field from the irradiated fuel.

The only common storage factors for the shrouds appear to be the presence of some amount of water or water vapor and a radiation field at least equal to the induced activity in the shroud. The exact amount of water present during storage is unknown except for the case of the element 7A insert which was stored in water. The next wettest storage condition was probably for element 7C. In this case, water was found in the fuel loading tube and contour rust lines were observed on the shroud. These lines were attributed to different water levels in the fuel loading tube during storage. There are no positive clues to the moisture conditions prevailing during the storage of element 5. However, a rust-colored corrosion product was on both the lead tube and shroud, and an x-ray analysis showed it to be $\text{Fe}_2\text{O}_3 \cdot \text{H}_2\text{O}$. From this evidence, it appears that elements 5 and 7C were exposed to water vapor or submerged in water to some depth for an unknown length of time during storage. Oxygen was common to all storage cases to the extent that it was dissolved in water or contained in the storage gas to a maximum of about 8.5% by volume.

Element 5 appeared to have suffered the most severe attack. There was localized intergranular attack at the outer surface of the cladding and extensive intergranular corrosion of the shroud and lead tube. The damage was so intense that the lead tube fractured during in-cell handling, and both the lead tube and shroud metallographic specimens crumbled during preparation. Next in order of severity of attack appeared to be the insert for element 7A. The bottom portion of the insert rusted badly while in the pool water, and a longitudinal fracture developed at the bottom while being sectioned for metallographic

examination. The fracture was intergranular. The extent of intergranular attack of element 7C was judged to be about the same as for the shroud of element 7A. The metallographic specimen obtained from the bottom of the element 7C shroud revealed a lack of grain boundary integrity although it was sporadic and observed in only three areas of the specimen. Elements 6 and 7B showed no outward signs of attack.

— The unusual severity of the intergranular corrosion of the element 5 shroud might be attributable to the presence of large amounts of water vapor in the loop during irradiation. The loop gas (helium) was initially dry, but a water leak occurred in a compressor during the test. The helium was not analyzed for water, but after two weeks of operation, the hydrogen content was 800 ppm. The hydrogen could have resulted from the reaction of water vapor with various high-temperature components and by radiolytic decomposition in the high-radiation field.

The effect of shroud temperature on the extent of intergranular attack is not clear from the observations. For instance, if the lower end of the shroud is assumed to operate at the average gas outlet temperature, the shroud for element 7A operated at the lowest temperature. It was 30 to 40% below the shroud temperatures of the other elements — all of which operated at about the same higher average temperature (see Table 2). This difference did not appear to influence the results significantly. However, the average temperature is not an indicator of possible short-duration high-temperature heat treatments which can sensitize the austenitic stainless steel in a few minutes or hours.

Time in storage and time delays after removal from storage did not appear to be major factors. As indicated in Table 2, the shroud for element 7C was in storage for 15 days and was extensively corroded, whereas the shroud for element 6 was stored for 31 days and was not attacked. Elements 7C and 6 were examined 46 and 44 days after irradiation, respectively. In all probability, the degree of attack differed because of distinct differences in the storage environment and not the storage time.

In general, the test element cladding appeared to be less susceptible than the shrouds to extensive intergranular corrosion. This might be attributed to decreased sensitization of the austenitic

stainless steel as the result of higher operating temperatures. It is also possible that after-heat produced from the irradiated fuel reduced water condensation on the clad surface during storage and thus prevented concentration of impurities by reevaporation.

Although intergranular corrosion was the predominate mode of failure, some transgranular corrosion with branching was observed, such as shown in Fig. 6. Transgranular cracks with branches are usually attributed to stress corrosion in austenitic stainless steels. However, the test element shrouds and inserts were not subjected to significant mechanical stresses and the high operating temperatures precluded any significant residual stresses. It is possible that the transgranular cracks observed in Fig. 6 resulted from local stresses created by the intergranular corrosion process.

RELEVANT LITERATURE

Stickler and Vinckier² have shown a direct relationship between the corrosion behavior and the morphology of the grain boundary carbide in austenitic stainless steels. These workers subjected type 304 stainless steel (0.038% C) specimens to a wide range of sensitizing heat treatments. They observed that at lower sensitizing temperatures (900 to 1200°F) grain boundary carbide formed predominately as a sheet of connected small particles. At higher sensitizing temperatures (1350 to 1500°F) the carbide occurred predominately as isolated dendritic particles (the term "dendritic" was assigned by Stickler and Vinckier²). They found that poor intergranular corrosion resistance was associated with the sheets and good resistance with the dendritic particles. (The intergranular corrosion tests were performed by immersing the specimens in Strauss solution: 100 g CuSO₄, 100 ml H₂SO₄, distilled H₂O to form 1 liter of test solution.) These authors were able to fully explain the intergranular corrosion behavior without postulating any grain boundary chromium depletion. They postulated that, "the corrosion is an electrochemical reaction between the carbide particles and the matrix which rapidly penetrates into specimens along grain boundaries when there is a continuous path provided by sheets of connected small carbide particles."³

²R. Stickler and A. Vinckier, Trans. Am. Soc. Metals 54, 362-80 (1961).

³Ibid., p. 362.

It is interesting to note that a fine and apparently continuous precipitate was observed along the grain boundaries in the metallographic specimen taken from the top portion of test element 7C (see Fig. 16). The estimated operating temperature of the cladding in this region was 1200°F. Near the midlength of this same element, the cladding temperature was higher and the intergranular precipitate appeared dendritic (see Fig. 17).

The intergranular attack of sensitized type 304 stainless steel by the Strauss solution is thought to be a series of local electrochemical attacks supported by the potential difference between the carbide and the less noble matrix. These localized attacks propagate along the sheet-type grain boundary carbides. The extent to which this process may be enhanced by radiation is not known.

The possible effects of radiation on metallic corrosion by various fluids have been treated extensively in a survey article by Stobbs and Swallow.⁴ In order to relate this work to the observed intergranular corrosion of the test elements, it is necessary to identify the corrosive fluid. One hypothesis is the formation of nitric acid by an irradiation-induced reaction between nitrogen and oxygen in the storage tube (tube contains approximately 91.5% N₂, 8.5% O₂, plus an unknown quantity of water vapor). This appears to be a valid hypothesis for the source of a corrosive fluid; however, it does not seem to account for the failure of the element 7A insert which was stored underwater. The nitrogen fixation process does not occur in aqueous solution, and the exposure time to air was less than 1 hr with the primary radiation source (test fuel element) already detached.

Water as the corrosive fluid may be a creditable hypothesis for explaining the attack of the element 7A insert if radiolysis at the grain boundaries is assumed to have an inefficient reverse reaction. Ordinarily, for a low ionization density case, the back reaction is readily catalyzed by the free radicals so no net decomposition occurs. However, Stobbs and Swallow⁴ point out that the reverse reaction can be retarded by impurities or by removing the hydrogen from the liquid

⁴J. J. Stobbs and A. J. Swallow, Metall. Rev. 7, 95-131 (1962).

phase. In this case, an oxidizing solution containing hydrogen peroxide and oxygen is possible. Such a solution could form the corrosive fluid. It is interesting to note that a corrosion product which appeared to be an oxide was observed in the intergranular failure of element 5 (see Fig. 7), and there was evidence of intergranular corrosion products in other components such as the insert for element 7A (see Fig. 10b).

Another effect that should be considered is the grain growth which is observed in certain regions of the type 304 stainless steel cladding following irradiation. This growth is readily apparent in Fig. 11. The extent to which the resulting grain boundaries may be subject to attack by a given corrosive fluid is unknown.

ADDITIONAL REMARKS

Because of the extensive intergranular corrosion of these test fuel elements, steps were taken to change the storage environment. These steps included the use of helium instead of nitrogen as the pressurizing gas (storage gas now contains approximately 57.5% He, 34% N₂, and 8.5% O₂). In addition, many extra precautions were taken to remove all traces of water and prevent any inleakage, and an effort was made to minimize storage time. The next four elements examined after the initiation of this change were in storage from 3 to 10 days (average of 6 days) as opposed to the previous storage time of 15 to 44 days (average of 26 days).

Since the above changes in the storage environment were made, there has been no new evidence of gross intergranular attack of the type 304 stainless steel test elements. Because there is still a large amount of nitrogen and oxygen in this new storage environment, it is believed that the steps taken to eliminate water vapor have been responsible for the improvement. It is conceded that the very short storage time might be a factor, but this was observed not to be the case for longer storage times.

CONCLUSIONS

From the observations reported in this document, it is concluded that the storage of sensitized, irradiated type 304 stainless steel in a high-humidity environment or underwater may lead to extensive intergranular corrosion. Admittedly, the evidence is fragmentary because it was obtained as a by-product of other experimentation, but the observations appear conclusive for the case of underwater storage. This is particularly important because of the intent of certain reactor projects, such as the EGCR project, to store spent fuel elements fabricated from type 304 stainless steel underwater.

It is believed that these observations are of significant interest to reactor metallurgists and of sufficient importance to warrant a careful experimental verification.

ACKNOWLEDGMENTS

This report represents only a portion of the postirradiation examinations that were performed on the EGCR prototype fuel elements discussed. The complete examination of these fuel elements was the responsibility of the Reactor Chemistry Division. These examinations were performed under the supervision of O. Sisman. The complete results were compiled by J. B. Morgan.

ORNL-3684
 UC-25 - Metals, Ceramics, and Materials
 TID-4500 (34th ed.)

INTERNAL DISTRIBUTION

1-3. Central Research Library	53. H. C. McCurdy
4. Reactor Division Library	54. J. R. McWherter
5-6. ORNL - Y-12 Technical Library	55-60. C. Michelson
Document Reference Section	61. E. C. Miller
7-26. Laboratory Records Department	62. J. F. Murdock
27. Laboratory Records, ORNL R.C.	63. P. Patriarca
28. R. J. Beaver	64. R. E. Reed
29. E. G. Bohlmann	65. H. W. Savage
30. Craig Brandon	66-71. J. L. Scott
31. J. A. Burka	72. R. L. Senn
32. J. A. Conlin	73. C. E. Sessions
33. F. L. Culler	74. O. Sisman
34. J. E. Cunningham	75. M. J. Skinner
35. J. H. DeVan	76. L. E. Stanford
36. I. T. Dudley	77. J. A. Swartout
37. J. L. English	78. J. W. Tackett
38. B. Fleisher	79. W. C. Thurber
39. J. H. Frye, Jr.	80. D. E. Tidwell
40. J. K. Franzreb	81. C. D. Watson
41. R. J. Gray	82. A. M. Weinberg
42. J. C. Griess	83. J. R. Weir
43. D. M. Hewette II	84. D. B. Trauger
44-46. M. R. Hill	85. M. S. Wechsler
47. C. E. Larson	86-105. G. D. Whitman
48-49. E. L. Long, Jr.	106. M. B. Bever (consultant)
50. T. S. Lundy	107. A. A. Burr (consultant)
51. H. G. MacPherson	108. J. R. Johnson (consultant)
52. H. E. McCoy, Jr.	109. A. R. Kaufmann (consultant)

EXTERNAL DISTRIBUTION

- 110. C. M. Adams, MIT
- 111. E. A. Aitken, GE, NMPO
- 112. A. J. Alexander, AEC, CANEL
- 113. G. M. Anderson, AEC, Washington
- 114. C. H. Armbruster, Wright-Patterson Air Force Base
- 115. W. K. Barney, KAPL
- 116. D. E. Baker, GE, Hanford
- 117. J. A. Basmajian, Los Alamos Scientific Laboratory
- 118. H. C. Brassfield, GE, NMPO
- 119. M. W. Burkhart, Westinghouse, Bettis Atomic Power Division
- 120. V. P. Calkins, GE, NMPO
- 121. W. Chernock, Combustion Engineering, Inc.
- 122. S. S. Christopher, AEC, Washington
- 123. T. D. Cooper, Wright-Patterson Air Force Base

- 124-125. D. F. Cope, AEC, ORO
126. D. M. Dayton, Battelle Memorial Institute
127. M. A. DeCrescente, Pratt & Whitney, CANEL
128. R. F. Dickerson, Battelle Memorial Institute
129. E. M. Douthett, AEC, Washington
130. Ersel Evans, GE, Hanford
131. W. C. Francis, Phillips Petroleum Company, Idaho Falls
132. N. Fuhrnam, United Nuclear Company
133. D. C. Goldberg, Westinghouse Astronuclear Laboratory
134. J. L. Gregg, Cornell University
135. D. H. Gurinsky, Brookhaven National Laboratory
136. R. Hall, Lewis Research Center
137. B. R. Hayward, Atomics International
138. E. E. Hoffman, GE, Cincinnati
139. W. Johnston, Atomics International
140. J. H. Kittel, Argonne National Laboratory
141. G. A. Last, GE, Hanford
142. J. A. Leary, Los Alamos Scientific Laboratory
143. L. J. Martel, KAPL
144. T. W. McIntosh, AEC, Washington
145. W. McNeish, Universal Cyclops
146. A. D. Miller, Pratt & Whitney, CANEL
147. T. A. Moss, NASA, Lewis Research Center
148. L. A. Neimark, Argonne National Laboratory
149. R. A. Noland, Argonne National Laboratory
150. R. G. Oehl, AEC, Washington
151. T. Pashos, GE, Vallecitos Atomic Laboratory
152. D. V. Ragone, General Atomic
153. L. M. Raring, Pratt & Whitney, CANEL
154. W. L. Rice, AEC, Washington
155. W. E. Roake, GE, Hanford
156. Louis Rosenblum, NASA, Lewis Research Center
157. F. A. Rough, Battelle Memorial Institute
158. F. C. Schwenk, AEC, Washington
159. A. A. Shoudy, APDA
160. J. Simmons, AEC, Washington
161. E. E. Stansbury, University of Tennessee
162. D. K. Stevens, AEC, Washington
163. A. Strasser, United Nuclear Corporation
164. W. Titus, Aerojet-General Nucleonics
165. J. M. Tobin, Westinghouse Electric Corporation
166. C. E. Weber, Atomics International
167. B. Weidenbaum, Vallecitos Atomic Laboratory
168. A. Weinberg, General Atomic
169. G. W. Wensch, AEC, Washington
170. M. J. Whitman, AEC, Washington
171. Research and Development Division, AEC, ORO
- 172-755. Given distribution as shown in TID-4500 (34th ed.) under Metals, Ceramics, and Materials category (75 copies - CFSTI)